Raman spectroscopic analysis of DEA 1.1 canine RBC membrane glyco protein and its application in canine blood typing

G. Kalaiselvi*, K.G. Tirumurugaan, G. Dhinakar Raj, K. Vijayarani, R. Baranidharan

Department of Animal Biotechnology, Madras Veterinary College, Chennai -7, TANUVAS, India.
*Corresponding author e-mail: kalaiselvigovindan1981@gmail.com

Journal of Livestock Science (ISSN online 2277-6214) 13: 194-200
Received on 31/5/22; Accepted on 27/7/22; Published on 3/8/22
doi. 10.33259/JLivestSci.2022.194-200

Abstract

Dog erythrocytic membrane antigen plays a major role for determining blood group. Structural and molecular characterization of erythrocytic membrane antigen improves the production of blood typing antisera, to study the auto antibody production in canine autoimmune haemolytic anemia. The proteins in the lipid domain arranged from the inside of the erythrocyte to the outside. The integral membrane proteins include membrane protein 3 visible in Coomassie Brilliant Blue-stained polyacrylamide gels. The erythrocyte cytoskeleton consists of spectrin, ankyrin, actin and protein 4.1 form a filamentous network under the lipid bilayer of erythroctic membrane. Most characteristic bands are associated with the CO =NH group referred to as amide A have NH stretching mostly found at 3500 cm^{-1} wave number. The amide B had NH stretching found at the region of 3100 cm^{-1} and amide I & III were used to estimate the secondary structure of proteins. Amide I mode which ranges from 1580 cm^{-1} to 1700 cm^{-1} and very sensitive to the backbone conformation and not affected by the side chains. Amide I band can be de convoluted with various sub-bands which directly correlate with various secondary structures The good intensity sharp peak at the level of 1468 cm^{-1} and 2034.694 cm^{-1} were taken for 2D analysis the CCD cts scale bar shows differences between DEA1.1 positive and negative dog erythrocytic membrane antigen.

Key words: Raman spectroscopy; Dog erythrocytic membrane antigen; Amide 1 Bands; blood grouping

Introduction

The raman spectroscopy has become an important tool for chemists, physicists, biologists and the raman spectral signatures of proteins, nucleic acids, lipids and carbohydrates shows significant results associated with disease diagnosis. The raman spectroscopy can be used to probe the secondary and tertiary structural changes occurring during thermal denaturation of protein and lysozyme as well as more complex biological systems like bacteria, tissues, cells, blood serum unique signature raman spectra shows difference in the relative composition of the biomolecules. Raman spectroscopy is an excellent tool to identify protein structure and various vibrational modes can be used for the analysis of peptide structure. The raman spectroscopy also useful for disease diagnosis and estimation of biological fluid composition.

The quantitative high-resolution microscopies, atomic force microscopy for recognition of senescence and identification of appropriate molecular markers and specific morphological changes associated with RBC senescence. The relationship between erythrocytes plasma membrane roughness and severe cytoskeleton defects and the progression of the RBCs' ageing and dramatic reduction and plasma membrane roughness was observed in cells that lost their membrane cytoskeleton integrity either temporarily or permanently. Specific membrane proteins induce the morphological alterations that ageing of RBC and role of band 3, spectrin, ankirin, and the proteins of the bands 4.1 and 4.2 structural protein remains unclear but the interactions of these proteins with the haemoglobin and lipid peroxidation for the induction of specific ageing patterns. The Raman spectro microscopy giving information about biochemical alterations associated to peculiar morphological changes of single cell but differential scanning calorimetry which give information about thermal stability of cell component and the denaturation or unfolding of specific cell components in various thermal transition. RBC aging were analysed by using differential scanning calorimetric technique and denaturation of bands 2, 4.1, and 4.2 will affects the hemoglobin stability and denaturation RBC major membrane proteins affects the hemoglobin and glycolysis enzymes causes oxygenation dynamics of hemoglobin. The progressive denaturation of the band 3 proteins seen during the ageing leads to production of met haemoglobin, and Hb denaturation and senescence of RBC (Jarolim *et al.*,1990, Girasole *et al.*, 2010, Kozlova *et al.*, 2013, Doty *et al.*,2017)

The Raman signal is producing a precise spectral sample fingerprint, unique to each atom, group of atoms or individual molecule. In this respect it is similar to the more commonly found FT-IR spectroscopy. Raman spectroscopy can be used to analyse aqueous solutions and the intensity of spectral features is directly proportional to the concentration of the particular species. Raman requires little or no sample preparation and use of a Raman microscope provides very high level of spatial resolution and depth discrimination. Raman has become a very powerful tool for analysis and chemical monitoring of biological samples. The improved Raman spectroscopy, especially in lasers, optics, detectors and data analysis makes this type of investigation easier. The sensitivity had been increased because of advances in optical filters and phonon detectors and single-channel detectors were replaced by CCD detectors and fluorescence was minimized by using red and infrared excitation in the 630–850 nm range. The problems with interpreting Raman data have been reduced with the availability of powerful software which was able to discriminate throughout statistical methods. Raman spectroscopy being a nondestructive and noninvasive method which will not disturb the studied system. The optical technique can provide rapid, objective and reproducible measurements on biological samples (Goodacre, *et.al*.,1998) Raman spectroscopy is particularly suitable for detection and analysis of the changes in molecular polarizability of biomolecules, changes involved in the modifications of proteins conformation in binding or interaction mechanisms. The well-resolved amide III band in the Raman spectrum has been used to determine precisely the secondary conformation of protein (Cai *et.al*.,2004). The spectral changes associated with aromatic amino acids such as tyrosine, phenylalanine, and tryptophan residues were also used to track some interactions induced by structural modifications. The main objective of this research is application of Raman spectroscopy for characterizing erythrocytic membrane antigen of DEA 1.1 positive and negative RBC and its application in blood grouping in future.

Materials and methods

The blood samples required for the present study were collected from registered blood donor dogs from Madras Veterinary College, canine blood bank, Chennai 7, Veterinary Peripheral Hospital, Madhavaram Milk Colony, Madhavaram and Centralized Clinical Laboratory, Madras Veterinary College, Chennai -7. Alvedia Easy Quick immuno-chromatographic strip test kits were used for typing DEA1. positive and negative blood samples. The DEA1.1 ghost membrane antigen was prepared as per the method described by Francesco Di Girolamo (2010) with slight modification. 5ml of DEA1.1canine blood was taken in a tube and initially the blood sample was centrifuged at 1500 rpm for 15 min at 4°C. The supernatant plasma and Buffy coats are removed and the RBC pellet was washed three times with PBS with 10 mM phenyl methyl sulfonyl fluoride protease inhibitor. The samples were

centrifuged at 800 rpm for 20 min at 4°C and the remaining leukocytes and platelets were completely removed and the numbers of RBCs were counted in haematology analyzer. The 2 X 10^{10} RBC concentration was used for ghost membrane preparation. The pellet was diluted 10 times with 150 mM of NaCl which contain 10mM of phenyl methyl sulfonyl fluoride protease inhibitor. The samples were continuously freeze thawed with LN2 for 4 times and centrifuged at 13000 rpm for 30 min at 4°C. The supernatant was removed and the pellet was again resuspended with 2 ml of 0.15% NaCl and shaken vigorously then centrifuged at 13000 rpm for 15 min and the supernatant was discarded. The lysed cell pellet was treated with 10 volumes of ice cold PBS containing 10mM of PMSF of 20 mM EDTA. The lysed cells were washed three times with the same buffer containing 10mM of NaOH until the pellet become white ghost. The centrifuged membranes were white, showing no traces of attached hemoglobin. The EDTA-lysed membrane preparations were then resuspended in the isotonic phosphate buffer with 10 mM of PMSF, 0.2 % OPG and 0.1% triton X 100 with 10 mM phenyl methyl sulfonyl fluoride. The protein concentration was estimated by using Bradford assay along with known concentration of BSA and stored at -80^{O} C. the membrane glycoprotein was extracted and the concentration of glycoprotein was estimated by phenol sulphuric acid assay. The instrument facilities utilized from centralized instrumentation laboratory Vels University, Pallavaram, Chennai. The Raman spectroscoscoy measurement was done based on the method described by Daniel *et al.*, (2008) The confocal hole was set to the minimum value. The dispersive system is comprised of a single grating with 600 groves/mm, and the Raman signal is collected thanks to a front illuminated CCD detector. 3 series of independent measurements were carried out for each samples and for each set, the Raman experiment was repeated 6 times to check the reproducibility of the measurement and to minimize the possible artifacts. Each spectrum was preprocessed with a 9-point Savitzky-Golay function corresponding to a denoising routine. The background corrected with a polynomial function. Raman maps were acquired with a DXR Thermo Fisher Scientific Raman Microscope by exciting the samples at 532 nm with a 2 mW power and a 50× objective. The measured spectral range was 300 to 5000 cm^{-1} and each spectrum resulted from 1 acquisition and 10 accumulations. The mapping resolution was set at 1 µm obtaining around 20 to 25 spectra per cell that have been averaged to produce a single mean spectrum for each cell. Analytical Parameters includes Large Scale Image Scan (Area): Points per Line: 100, Lines per Image: 100, Scan Width [µm]: 10.000, Scan Height [µm]: 10.000, Scan Speed [s/Line]: 30.000, Integration Time [s]: 0.3. The UHTS300S_GREEN_NIR: Excitation Wavelength [nm]: 532.335, Grating: G2: 600 g/mm BLZ=500nm, Center Wavelength [nm]: 596.998, Spectral Center [rel. 1/cm]: 1468 &2034.694 was used at the time of measurement.

Results and discussion

Raman spectroscopy is an excellent tool to identify protein structure and various vibrational modes can be used for the analysis of peptide structure. Most characteristic bands are associated with the CO = NH group, referred to as amide A have NH stretching mostly found at 3500 cm-1 wave number, amide B had NH stretching found at the region of 3100 cm -1 and amide I & III were used to estimate the secondary structure of proteins. Amide I mode which ranges from 1580 cm-1 to 1700 cm-1 and very sensitive to the backbone conformation and not affected by the side chains. Amide I band can be deconvoluted with various sub-bands which directly correlate with various secondary structures. Amide III band found 1200 cm^{-1} –1300 cm^{-1} arises from C–N stretching coupled with N–H bending vibrations (Lippert *et al.*, 1976, Williams 1986).

The spectra of the isolated ghost cells membranes showed bands at 1110 cm^{-1}, 1340 cm^{-1}, 1420 cm^{-1} and 1445 cm^{-1} were attributed by hydrocarbon chains of the fatty acids with a possible small contribution from the CH2 groups of cholesterol. Raman spectroscopy was used to study the protein components of RBC ghosts the protein fraction contained 40–55% a-helix with little b-configuration and that 55–65% of the hydrophobic side chain content of the phospholipid were in the all-trans rigid configuration. All Raman modes were assigned to either protein or phospholipid at 488 nm excitation with no suspected contribution from cholesterol (Bulkin *et al.*,1972). The 2D Raman correlation spectroscopy used to investigate age-related disintegration of RBCs were demonstrated by raman spectroscopy at 785 nm excitation to study the donor-dependent build-up of lactate in the supernatant of stored units and correlations between lactate release and specific donor characteristics, such as gender and age (Atkins *et al.*, 2015).

Raman spectroscopy used as a diagnostic tool to detect minute changes in the plasma protein albumin, fibrinogen, cytochrome C and vitamin B12 concentrations in bio fluids as well as biopsy samples for disease diagnosis. High molecular weight proteins from low molecular weight proteins were separated by using ion exchange chromatography. The mild sonication of samples improved the dispersion of fibrinogen and the standardization of measurement protocol and other experimental parameters depends on concentration of proteins, purity of protein and the chemo metric methods used to build the prediction model which influences the of Raman spectroscopy analysis (Mitchell *et al.*,2014, Blades *et al.*,2015). Raman spectra were plotted in units of intensity versus Raman shift in wave numbers (cm^{-1}). The good intensity sharp peak at the level of 1468cm^{-1} and 2034.694 cm^{-1} were taken for 2D analysis (Figure 1, 2 & 7, 8). The CCD cts scale bar showed differences between DEA1.1 positive and negative membrane glycoprotein (Figure 3, 4 & 9, 10) and that area selected for 2D and 3D analysis for identification of function group and α helix and β sheets structure (stretching symmetric vibration of C=C, C=C functional group structure (ν (C=H) functional group identified) and stretching asymmetric (CH2)δ(CH3) identified (Figure 5, 6 & 11, 12).

The previous study showed spectra of the isolated ghost cells membranes showed bands at 1110 cm^{-1}, 1340 cm^{-1}, 1420 cm^{-1}, and 1445 cm^{-1} were attributed by hydrocarbon chains of the fatty acids with a possible small contribution from the CH2 groups of cholesterol. Raman spectroscopy was used to study the protein components of RBC ghosts the protein fraction contained 40–55% a-helix with little b-configuration and that 55–65% of the hydrophobic side chain content of the phospholipid were in the all-trans rigid configuration. All Raman modes were assigned to either protein or phospholipid at 488 nm excitation with no suspected contribution from cholesterol (Bulkin *et al.*,1972). The 2D Raman correlation spectroscopy used to investigate age-related disintegration of RBCs were demonstrated by raman spectroscopy at 785 nm excitation to study the donor-dependent build-up of lactate in the supernatant of stored units and correlations between lactate release and specific donor characteristics, such as gender and age.

Raman spectroscopy for clinical applications primarily been focused on spectral differences in the fingerprint region (up to 1800 cm^{-1}), some studies have investigated the diagnostic utility of spectral features in the high-wavenumber (2200–4500 cm^{-1}) in this range, strong features of lipids, proteins and water may be observed. Many studies have demonstrated the potential of high wavenumber Raman spectroscopy alone or in combination with fingerprint Raman methods to diagnose and classify disease in vivo condition (Bergholt *et al*., 2016)

Raman spectroscopy selected as a method for estimation of the age of bloodstain aged up to one week combined with a two-dimensional correlation spectroscopy method and which able to differentiate between fresh or old bloodstains by utilizing a developed regression model (Doty *et al*.2016). Fluorescence lifetime measurements utilized to determine the time since the deposition of bloodstains. The experiment was carried out by using human blood obtained from 6 donors. Decrease in the fluorescence lifetime within the first 91 hrs of deposition, after which the fluorescence lifetime plateau which illustrate a clear distinction between fresh and old bloodstains (Mc Shine *et al.* 2017). Amide III band found 1200 cm^{-1} –1300 cm^{-1} arises from C–N stretching coupled with N–H bending vibrations (Lippert *et al.*, 1976, Williams 1986)

In this study, the measured spectral range was 300 to 5000 cm−1 and each spectrum resulted from 10 s acquisition and 10 accumulations with laser wavelength 532 nm @2mW. All the spectra were baseline corrected. The mapping resolution was set at 1 μm obtaining around 20 to 25 spectra per cell that have been averaged to produce a single mean spectrum for each cell. Raman spectra are plotted in units of intensity versus Raman shift in wave numbers (cm^{-1}). The good intensity sharp peak at the level of 1468 cm^{-1} and 2034.694 cm^{-1} taken for 2D analysis the CCD cts scale bar shows differences between DEA1.1 positive and negative and that area selected for 2D and 3D analysis for identification of function group and α helix and β sheets structure (stretching symmetric vibration of C=C, C=C functional group structure (ν (C=H) functional group identified) and stretching asymmetric (CH2)δ(CH3) identified. However this is first time we analyzed canine erythrocytic membrane glycoprotein by using raman spectroscopy and tried raman spectroscopy for blood grouping. The DEA 1.1 positive and negative membrane glycoprotein showed significant differences in the composition of membrane glycoprotein but however in-depth detailed further studies were needed.

Raman spectroscopy images

DEA1.1 positive membrane glycoprotein

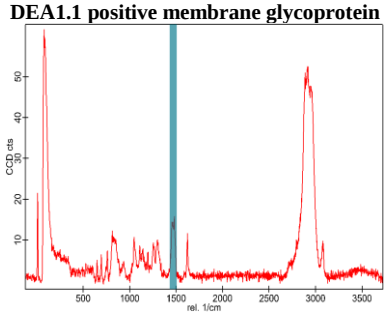

Figure 1: Raman spectra are plotted in units of intensity versus Raman shift in wave numbers (cm^{-1}) from 500 cm $^{-1}$ to 3500 cm $^{-1}$
The good intensity sharp peak at the level of 1468 cm^{-1} taken for 2D analysis

DEA1.1 Negative membrane glycoprotein

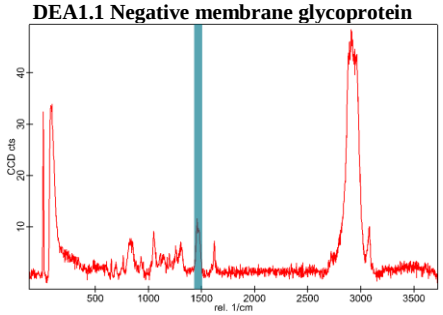

Figure 2: Raman spectra are plotted in units of intensity versus Raman shift in wave numbers (cm^{-1}) from 500 cm $^{-1}$ to 3500 cm $^{-1}$
The good intensity sharp peak at the level of 1468 cm^{-1} taken for 2D analysis

DEA1.1+++SCALE BAR

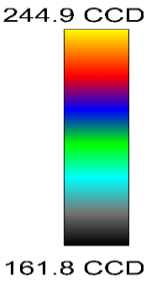

Figure 3: The CCCD cts scale bar of DEA1.1 positive membrane glycoprotein showed the ranges between 161.8 to 244.9.

DEA1.1-----SCALEBAR

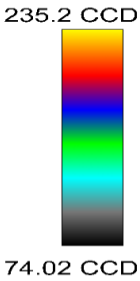

Figure 4 : The CCCD cts scale bar of DEA1.1 negative membrane glycoprotein showed 74.02 to 235.2

2D and 3D images of DEA1.1 +++

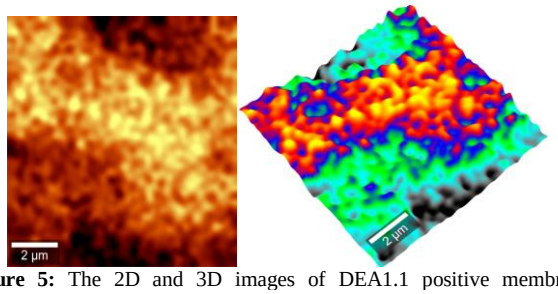

Figure 5: The 2D and 3D images of DEA1.1 positive membrane glycoprotein showed high concentration of function group and α helix and β sheets structure stretching symmetric vibration of C=C, C=C functional group and stretching asymmetric (CH2)δ(CH3)

2D image DEA1.1 ----

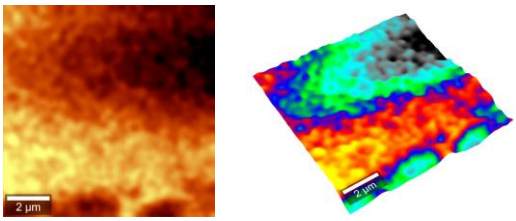

Figure 6: The 2D and 3D images of DEA1.1 positive membrane glycoprotein showed comparatively less concentration of function group and α helix and β sheets structure stretching symmetric vibration of C=C, C=C functional group and stretching asymmetric (CH2)δ(CH3)

DEA1.1 positive

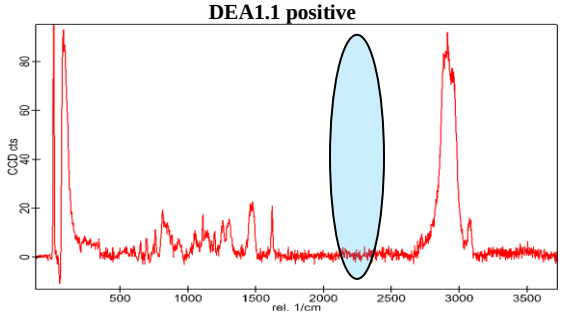

Figure 7: Raman spectra are plotted in units of intensity versus Raman shift in wave numbers (cm^{-1}) from 500 cm $^{-1}$ to 3500 cm $^{-1}$. The peak at the level of 2034.694 cm^{-1} taken for 2D analysis

DEA1.1 Negative

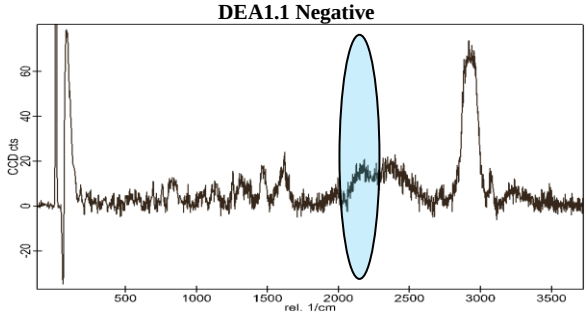

Figure 8: Raman spectra are plotted in units of intensity versus Raman shift in wave numbers (cm^{-1}) from 500 cm $^{-1}$ to 3500 cm $^{-1}$. The peak at the level of 2034.694 cm^{-1} taken for 2D analysis

DEA1.1+++SCALE BAR

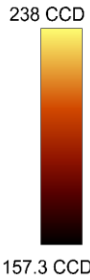

Figure 9: The CCCD cts scale bar of DEA1.1 positive membrane glycoprotein showed the ranges between 157.3 to 238 CCD cts

DEA1.1-----SCALEBAR

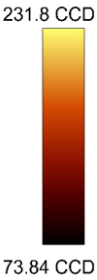

Figure 10: The CCCD cts scale bar of DEA1.1 positive membrane glycoprotein showed the ranges between 73.84 to 231.8 CCD cts

2D image DEA1.1 +++

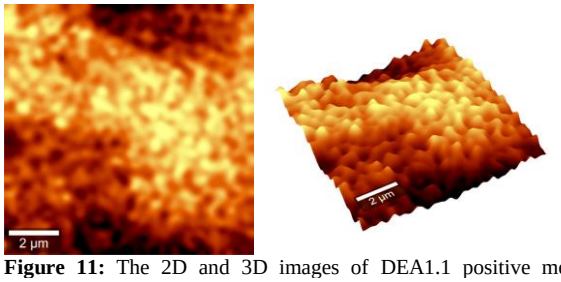

Figure 11: The 2D and 3D images of DEA1.1 positive membrane glycoprotein showed high concentration of function group and α helix and β sheets structure stretching symmetric vibration of (ν (C=H) functional group

2D image DEA1.1 ----

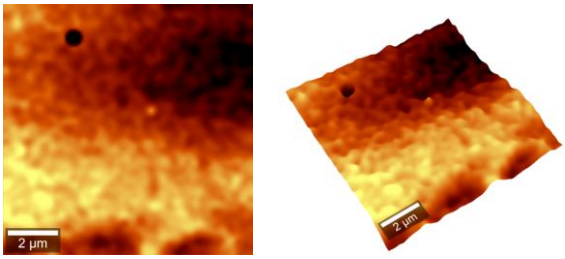

Figure 12: The 2D and 3D images of DEA1.1 positive membrane glycoprotein showed comparatively low concentration of function group and α helix and β sheets structure stretching symmetric vibration of (ν (C=H) functional group

Acknowledgement

Authors are thankful to TANUVAS and Vels University Pallavaram, Chennai for providing necessary facilities.

References

1) Bergholt MS, Lin K, Wang J, Zheng W, Xu H, Huang Q, Ren JL, Ho KY, Teh M, Srivastava S, Wong B, Yeoh KG, Huang Z. 2016. Simultaneous fingerprint and high wave number fiber optic Raman spectroscopy enhances real time in vivo diagnosis of adenomatous polyps during colonoscopy Journal of Biophotonics. 9(5): 542-550
2) Blades MW, Turner RFB 2015. Raman Spectroscopy of Stored Red Blood Cells: Evaluating Clinically-Relevant Biochemical Markers in Donated Blood'. Proc. SPIE –Clinical and Biomedical Spectroscopy and Imaging IV. 9537: 95370X
3) Bulkin BJ 1972. Raman Spectroscopic Study of Human Erythrocyte Membranes. Biochimica et Biophysica Acta - Biomembranes. 274(2): 649–651
4) Cai S and Singh BR, 2004. A distinct utility of the amide III infrared band for secondary structure estimation of aqueous protein solutions using partial least squares methods, Biochemistry, 43: 2541–2549

5) Daniel P, Picart P, Bendriaa L et al 2008. Effects of toxic organotin compounds on bacteria investigated by micro- Raman spectroscopy, Spectroscopy Letters:, 41(1):19–28.
6) Doty KC, Muro CK, Lednev IK, 2017. Predicting the time of the crime: Bloodstain aging estimation for up to two years, Forensic Chemistry 5 1–7.
7) Francesco DG, Ponzi M, Crescenzi M, Alessandroni J and Guadagni F, 2010. A simple and effective method to analyze membrane proteins by SDS-PAGE and MALDI Mass Spectrometry. Anticancer Research 30: 1121-1130.
8) Girasole M, Pompeo G, Cricenti A, et al. 2010. The how, when, and why of the aging signals appearing on the human erythrocyte membrane: an atomic force microscopy study of surface roughness. Nanomedecine: Nanotechnology, Biology and Medecine. 6(6):760-768.
9) Goodacre R, Timmins EM, Burton R et al., 1998. Rapid identification of urinary tract infection bacteria using hyperspectral whole-organism fingerprinting and artificial neural networks, Microbiology, 144: 1157–1170.
10) Jarolim P, Lahav M, Liu SC, Palek J 1990. Effect of hemoglobin oxidation products on the stability of red cell membrane skeletons and the associations of skeletal proteins: correlation with a release of hemin. Blood 76(10):2125-2131.
11) Kozlova EK, Chernysh AM, Moroz VV, Kuzovlev AN 2013. Analysis of nanostructure of red blood cells membranes by space Fourier transform of AFM images. Micron (Oxford, England: 1993). 44: 218-227.
12) Lippert D, Tyminski and Desmeules PJ, 1976. Determination of the secondary structure of proteins by laser Raman spectroscopy, Journal of the American Chemical Society, 98: 7075–7080.
13) Mc Shine, Suhling K, Beavil A, Daniel B, Frascione N. 2017, The applicability of fluorescence lifetime to determine the time since the deposition of biological stains, Analytical Methods, 9: 2007–2013.
14) Mitchell AL, Gajjar KB, Theophilou G, Martin FL, Martin-Hirsch PL, 2014. Vibrational spectroscopy of biofluids for disease screening or diagnosis: Translation from the laboratory to a clinical setting, Journal of Biophotonics, 7(3-4), 153-165.
15) Williams RW. 1986. Protein Secondary Structure-Analysis Using Raman Amide-I and Amide-III Spectra, Methods Enzymology 130: 311–331.